

Available online at [www.sciencedirect.com](http://www.sciencedirect.com)

ScienceDirect

journal homepage: [www.jfda-online.com](http://www.jfda-online.com)

## Original Article

# Preparation, characterization, and antimicrobial activity of nanoemulsions incorporating citral essential oil



Wen-Chien Lu <sup>a</sup>, Da-Wei Huang <sup>b</sup>, Chiun-C.R. Wang <sup>c</sup>, Ching-Hua Yeh <sup>d</sup>,  
Jen-Chieh Tsai <sup>d</sup>, Yu-Ting Huang <sup>e</sup>, Po-Hsien Li <sup>d,\*</sup>

<sup>a</sup> Department of Food and Beverage Management, Chung-Jen Junior College of Nursing, Health Sciences and Management, Chia-Yi City, Taiwan, ROC

<sup>b</sup> Department of Food and Beverage Management, China University of Science and Technology, Taipei City, Taiwan, ROC

<sup>c</sup> Department of Food and Nutrition, Providence University, Shalu, Taichung, Taiwan, ROC

<sup>d</sup> Department of Medicinal Botanical and Health Applications, Da-Yeh University, Dacun, Changhua, Taiwan, ROC

<sup>e</sup> Institute of Food Science and Technology, National Taiwan University, Taipei, Taiwan, ROC

## ARTICLE INFO

## Article history:

Received 27 October 2016

Received in revised form

12 December 2016

Accepted 13 December 2016

Available online 14 February 2017

## Keywords:

antimicrobial activity

citral

mixed surfactant

nanoemulsions

## ABSTRACT

Citral is a typical essential oil used in the food, cosmetic, and drug industries and has shown antimicrobial activity against microorganisms. Citral is unstable and hydrophobic under normal storage conditions, so it can easily lose its bactericide activity. Nanoemulsion technology is an excellent way to hydrophilize, microencapsulate, and protect this compound. In our studies, we used a mixed surfactant to form citral-in-water nanoemulsions, and attempted to optimize the formula for preparing nanoemulsions. Citral-in-water nanoemulsions formed at  $S_o$  0.4 to 0.6 and ultrasonic power of 18 W for 120 seconds resulted in a droplet size of < 100 nm for nanoemulsions. The observed antimicrobial activities were significantly affected by the formulation of the nanoemulsions. The observed relationship between the formulation and activity can lead to the rational design of nanoemulsion-based delivery systems for essential oils, based on the desired function of antimicrobials in the food, cosmetics, and agrochemical industries.

Copyright © 2017, Food and Drug Administration, Taiwan. Published by Elsevier Taiwan LLC. This is an open access article under the CC BY-NC-ND license (<http://creativecommons.org/licenses/by-nc-nd/4.0/>).

\* Corresponding author. Department of Medicinal Botanical and Health Applications, Da-Yeh University, No.168, University Rd., Dacun, Changhua 51591, Taiwan, ROC.

E-mail address: [pohsien@mail.dyu.edu.tw](mailto:pohsien@mail.dyu.edu.tw) (P.-H. Li).

<http://dx.doi.org/10.1016/j.jfda.2016.12.018>

1021-9498/Copyright © 2017, Food and Drug Administration, Taiwan. Published by Elsevier Taiwan LLC. This is an open access article under the CC BY-NC-ND license (<http://creativecommons.org/licenses/by-nc-nd/4.0/>).

## 1. Introduction

Nanoemulsions are a class of emulsions with droplet sizes from 20 nm to 100 nm [1]. Because of the small droplet size, nanoemulsions appear transparent or translucent and are more stable with respect to creaming, coalescence, flocculation, and Ostwald ripening than convention emulsions [2]. The physicochemical properties of nanoemulsions are interesting for practical applications because of the small droplet size and long-term stability. Nanoemulsions are used in agrochemicals in pesticide drug-delivery formulas [3], in cosmetics as drug carriers for personal care or skincare products [4], and in pharmaceuticals as matrices for encapsulation of the bioactive compounds, which are desirable for alcohol-free formulation [5].

The best nanoemulsion droplets in emulsions are prepared with the optimal hydrophilic-lipophilic balance (HLB) and optimal surfactant concentration [6]. The proper HLB value of the surfactants is important for the formation of the emulsion. Nanoemulsions are usually formulated to enhance stability by use of a mixed surfactant because of the broad-chain length distribution. Vitamin E-enriched nanoemulsions have been reported by adjusting the HLB values of the surfactants with Tween 20, 40, 60, 80, and 85 [7]. Nanoemulsions containing astaxanthin prepared with a mixed surfactant have a smaller droplet size and a narrower size distribution than regular emulsions [8].

The formation of nanoemulsions is controlled by the relationship between droplet disruption and droplet coalescence. The ultrasonic processor applies excellent shear force for droplet disruption, and the rate of droplet coalescence is determined by the mixed surfactant and the concentration [9]. There are two main mechanisms operating during ultrasonic emulsification [10]. First, an acoustic field produces interfacial waves to break the disperse phase into the continuous phase. Second, the formation of acoustic cavitation is used to collapse microbubbles into droplets of nanometric size by pressure fluctuations.

The surfactants used in this study—Span 85 and Brij 97—are commonly used as emulsion surfactants in a wide range of food, cosmetic, and pharmaceuticals products. Nanoemulsions offer significant potential as functional ingredients in foods, cosmetic, and pharmaceuticals products because of their effectiveness to deliver flavors and aroma with their increased surface area and as mechanisms for delivering hydrophobic biocompounds. Therefore, it would be advantageous to formulate nanoemulsions with mixed surfactants, which have become widely acceptable in formulations of these types [11]. Brij-type surfactants possess a branched hydrophilic region of three polyoxyethylene chains substituted with a sorbitan ring, and Span-type surfactants have a large head group that can potentially aggregate at the oil/water (o/w) interface and form a hydrophobic region.

Citral (3, 7-dimethyl-2, 6-octadienal) is a monoterpene that occurs naturally in herbs, plants, and citrus fruits [12]. Citral possesses antifungal activity and bactericidal [13], insecticidal [14], deodorant, expectorant, appetite stimulating, and spasmolytic properties; it has weak diuretic and anti-inflammatory effects [15]. However, citral is susceptible to

oxidative degradation, which results in the loss of antimicrobial activity under normal storage conditions. Citral is also insoluble in water at neutral pH; therefore, nanoemulsion technology appears to be a good way to microencapsulate, solubilize, and protect this compound.

Nanoemulsion-based delivery systems with incorporated constituents significantly increasing the antimicrobial activity compared with nonencapsulated systems have promise [16–18]. The systems can increase the concentration of the bioactive compounds in areas where microorganisms are preferably located. The main objective of this study was to investigate the optimal conditions for preparing citral-in-water nanoemulsions with mixed surfactants using ultrasonic emulsification. Additionally, we evaluated the antimicrobial activity of citral nanoemulsions against bacteria.

## 2. Materials and methods

### 2.1. Materials

The citral (mixture of cis- and trans-isomers, 95% pure, of plant origin) used in this study was obtained from Merck (Darmstadt, Germany). Reagent grade Span 85 (sorbitane trioleate) and Brij 97 [polyoxyethylene (10) oleyl ether] with average HLB values of 1.8 and 12.0, respectively, were from Sigma (Deisenhofen, Germany). The ethylene glycol (C<sub>2</sub>H<sub>6</sub>O<sub>2</sub>, M.W. = 62 g/mol), used as a cosolvent in the emulsion system, was from Merck. The water used in this study was deionized and filtered using a Milli-Q system (Millipore Corp., Molsheim, France).

### 2.2. Nanoemulsion preparation

Nanoemulsions consisted of citral, a mixed surfactant, deionized water, and a cosolvent. The concentration of citral was fixed in 10%, and the HLB values of the mixed surfactant varied from 2 to 12. The HLB values of the mixed surfactant were calculated as follows:  $HLB_{mix} = HLB_S \cdot S\% + HLB_P \cdot P\%$ , where  $HLB_S$ ,  $HLB_P$ , and  $HLB_{mix}$  are the HLB values for Span 85, Brij 97, and the mixed surfactants, respectively, and S% and P% are the mass percentages of Span 85 and Brij 97 in the mixed surfactants, respectively. The HLB value of the surfactants was considered to be the algebraic average of the HLB value of the individual surfactant. The ratio of mixed surfactant to citral was expressed by the ratio  $S_o$ . The cosolvent concentration was fixed at 1%.

All emulsions were prepared in two stages. The coarse emulsion was obtained using a Polytron (PT-MR 3000, Kinematica AG, Littau, Switzerland), and then further emulsified with an ultrasonic process. Coarse emulsions containing different compositions were prepared at the highest speed for 10 minutes with a sample volume of about 30 mL each time. Ultrasonic emulsification involved use of a 20-kHz Sonicator 3000 (Misonix Inc., Farmingdale, NY, USA) with a 20-mm diameter tip horn. The tip of the horn was positioned symmetrically in the coarse emulsion, and the experiment was initiated at various preset ultrasonic nominal powers (6–51 W) for 30300 seconds and controlled by the device software. During emulsification, the difference in temperature

from the initial coarse emulsions to final emulsion was not more than 20°C. Each experiment was performed in triplicate.

### 2.3. Experiment design

Response surface methodology was used to systematically investigate the effect of the effect of the independent variables ultrasonic power ( $X_1$ ), time ( $X_2$ ), and  $S_o$  ratio ( $X_3$ ) on droplet size of citral nanoemulsions. The experiments involved the central composite design with a 20 factorial and star design with three central points as indicated in Table 1. Individual experiments were performed in random order.

### 2.4. Droplet size determination

Emulsion droplet size was determined by dynamic light scattering with a Nanotracer 150 system (Microtrac, Inc., Montgomeryville, PA, USA). To avoid multiple scattering effects, all emulsion samples were diluted to 10% with deionized water before measurement. Information about emulsion droplet size was obtained by a best fit between the theoretical light scattering and measured droplet size distribution. Emulsion droplet size was estimated by the average of three measurements and is presented as the mean diameter of the volume distribution (MN)

$$MN = \frac{\sum V_i d_i}{\sum V_i}, \quad (1)$$

where  $V_i$  is the volume percent between droplet sizes, and  $d_i$  is the droplet diameter.

### 2.5. Encapsulated ratio of citral

A 1-mL sample was dissolved in 20-mL deionized water in glass tubes and 10 mL of hexane was added, followed by

mixing with a mixer for 1 minute. Citral encapsulated in the nanoemulsions was extracted with hexane by heating the sample in glass tubes at 45°C in a water bath for 20 minutes with intermittent mixing. The tubes were cooled to room temperature and hexane was separated from the aqueous phase by centrifugation at 4000 rpm for 20 minutes. The amount of citral present in hexane was quantified by measuring absorbance by spectrophotometry at 252 nm. The encapsulated ratio was calculated as follows:

$$\text{Encapsulated ratio (\%)} = \frac{\text{Amount of encapsulated citral}}{\text{Total amount of added citral}} \quad (2)$$

### 2.6. Transmission electron microscope analysis

The morphology of the citral nanoemulsions was visualized with transmission electron microscopy (TEM). Samples (50  $\mu$ L) were added to 200-mesh formvar-coated copper TEM sample holders (EM Sciences, Hatfield, PA, USA), then negatively stained with 50  $\mu$ L of 1.5% (weight/volume) phosphotungstic acid for 10 minutes at room temperature. Excess liquid was blotted with Whatman filter paper. The TEM samples were observed under a JEOL JSM-1200 EX II transmission electron microscope (Peabody, MA, USA) equipped with a 20- $\mu$ m aperture at 67 kV.

### 2.7. Time stability

The stability of citral nanoemulsions was determined by measuring the change in droplet size during 14 days of storage at room temperature.

### 2.8. Microbial inactivation tests

The following bacterial strains were used in the antimicrobial assays: *Staphylococcus aureus* [American Type Culture Collection (ATCC) 27690], *Escherichia coli* (ATCC 23815), *Pseudomonas aeruginosa* (ATCC 15442), *Enterococcus faecalis* (ATCC 29212), *Salmonella typhimurium* (ATCC 14028), and *Listeria monocytogenes* (ATCC 19113). All strains were obtained from the Taiwan Bioresource Collection and Research Center (Hsinchu, Taiwan). The antimicrobial study involved the disc diffusion method according to the National Committee of Clinical Laboratory Standards protocol. First, agar plates were inoculated with a standardized test microorganism. Then, filter paper discs containing the antimicrobial agent at an appropriate concentration were placed on the agar surface. Petri dishes were incubated under suitable conditions. After incubation, the antimicrobial agent diffuses into the agar and inhibits germination and growth of the test microorganism, then the diameters of inhibition growth zones were measured. In this study, sulfazotrin discs were used as the positive control. Bacterial strains were inoculated in the stationary phase on nutrient agar plates, and citral nanoemulsions were dispensed for intimate contact. The plates were incubated at 35°C for 24 hours, then examined for growth of bacteria directly underneath and around the samples. The inhibition zones developed in and around the sample indicate the antimicrobial activity. The experiment was repeated five times.

**Table 1 – Central composite experimental design of response surface methodology.**

Experiment number	Independent variables		
	$X_1$	$X_2$	$X_3$
1	12	90	0.4
2	24	90	0.4
3	12	150	0.4
4	24	150	0.4
5	12	90	0.8
6	24	90	0.8
7	12	150	0.8
8	24	150	0.8
9	6	120	0.6
10	30	120	0.6
11	18	60	0.6
12	18	180	0.6
13	18	120	0.2
14	18	120	1.0
15	18	120	0.6
16	18	120	0.6
17	18	120	0.6
18	18	120	0.6
19	18	120	0.6
20	18	120	0.6

### 2.9. Statistical analysis

Results are given as mean  $\pm$  standard deviation. Statistical analysis involved one-way analysis of variance followed by Duncan's new multiple range tests. Differences were considered statistically significant at  $p < 0.05$ .

## 3. Results and discussion

### 3.1. Encapsulated ratio of citral under different HLB values

The nanoemulsions were prepared by using a mixed surfactant composed of Span 85 and Brij 97 under different HLB values. The HLB values of the mixed surfactants are a key factor in the formation of emulsion droplets. During the formation of an o/w emulsion, the lipophilic surfactants have greater affinity to the dispersed droplets in the emulsion than the hydrophilic surfactant. A proper HLB values is necessary to maintain the equilibrium of the oil and water phases. With an optimal HLB value, the newly formed droplets are stabilized during the emulsification and their droplet size is maintained. Figure 1 shows the effect of HLB values on the visual appearance of the emulsion. The emulsions appear to be opaque (white) at HLB values of 2 to 10 and are transparent or translucent at HLB value 12.

Studies have indicated that emulsion droplet size has a significant effect on the encapsulation efficiency of different core materials [19–21]. Reducing the emulsion droplet size can result in higher retention of encapsulated components in emulsion systems. However, the use of nanoemulsions in encapsulation of oils and flavors is rare in the literature. The encapsulated ratio of citral in nanoemulsions under different HLB values we obtained is shown in Table 2. The encapsulated ratio increased with increasing HLB value. With HLB value of 2, the droplet size was 410 nm and the citral encapsulated ratio was 64.3%, and with the HLB value increased to 12, the droplet was the smallest 28 nm, and the citral encapsulated ratio was 82.8%. Our results agreed with the literature, finding the retention of core materials higher for small than large emulsion droplets, and the citral retention in all nanoemulsion formulas was higher than 60%. The greater retention of flavor in small emulsion droplets is related to the reduced mean diameter of volume surface, which can enhance the modification of spherical interface organization and increase the interfacial area to govern the partition of aroma compounds in emulsions [20].

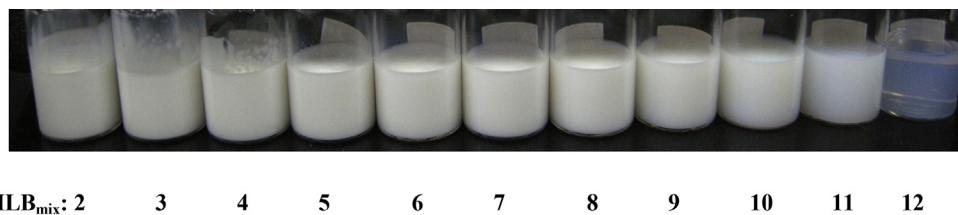


**Figure 1** – Effect of hydrophilic-lipophilic balance (HLB) values on the visual appearance of the nanoemulsions prepared by ultrasonic emulsification ( $S_o = 0.6$ ; ultrasonic power = 18 W; ultrasonic time = 120 seconds).

**Table 2** – Effect of HLB values on droplet size and citral encapsulated ratio in nanoemulsions. ( $S_o$  ratio = 0.6; ultrasonic power = 18 -W; ultrasonic time = 120 s).

No.	HLB <sub>mix</sub>	Emulsion droplet size (nm)	Encapsulated ratio (%)
1	2	410 <sup>a</sup> $\pm$ 21.8	64.3 <sup>e</sup> $\pm$ 1.6
2	3	402 <sup>a</sup> $\pm$ 17.5	66.7 <sup>d</sup> $\pm$ 1.7
3	4	355 <sup>b</sup> $\pm$ 12.7	67.9 <sup>c,d</sup> $\pm$ 2.2
4	5	279 <sup>c</sup> $\pm$ 11.8	68.3 <sup>c</sup> $\pm$ 1.3
5	6	256 <sup>c</sup> $\pm$ 6.1	70.2 <sup>c</sup> $\pm$ 3.4
6	7	216 <sup>d</sup> $\pm$ 1.8	72.1 <sup>b,c</sup> $\pm$ 3.2
7	8	185 <sup>e</sup> $\pm$ 6.3	73.9 <sup>b</sup> $\pm$ 4.1
8	9	126 <sup>f</sup> $\pm$ 1.4	75.1 <sup>b</sup> $\pm$ 3.9
9	10	90 <sup>g</sup> $\pm$ 0.9	78.2 <sup>a,b</sup> $\pm$ 3.7
10	11	67 <sup>h</sup> $\pm$ 0.3	82.2 <sup>a</sup> $\pm$ 2.9
11	12	28 <sup>i</sup> $\pm$ 0.4	82.8 <sup>a</sup> $\pm$ 4.1

<sup>a–i</sup> Means with different letters within the same column differed significantly ( $p < 0.05$ ). Values are mean  $\pm$  standard deviation ( $n = 3$ ).  
HLB = hydrophilic-lipophilic balance.

### 3.2. Optimization of conditions for preparing citral nanoemulsions

To realize the effect of the independent variables on dependent ones, we generated surface response and contour plots by varying two of the independent variables within the experimental range while holding another constant at the central point. Thus, Figure 2A was generated by varying the ultrasonic power and time in the emulsion while holding  $S_o$  ratio at 0.6. In our study, citral nanoemulsions were prepared by two steps. The first step involved preparing a coarse emulsion with droplet size of about 20  $\mu$ m by Polytron. Then, ultrasound was used to further decrease the droplet size to obtain the smallest droplet size. Droplets reached a minimum size at ultrasonic power of 18 W and ultrasonic time of 120 seconds, but in the other experimental design group, there were no evident change of droplet size at lower or higher ultrasonic power. The phenomenon of overprocessing may occur during ultrasonic emulsification, caused by an increase in droplet coalescence of emulsion at the higher ultrasonic power [21]. A similar trend between emulsion droplet size and ultrasonic power was observed for nanoemulsions composed of flaxseed oil, water, and Tween 40 [9].

Figure 2B was generated by varying the  $S_o$  ratio and ultrasonic time while holding ultrasonic power at 18 W. Ultrasonic time could affect the rate of adsorption of surfactants to the droplet surface and the droplet size distribution of newly

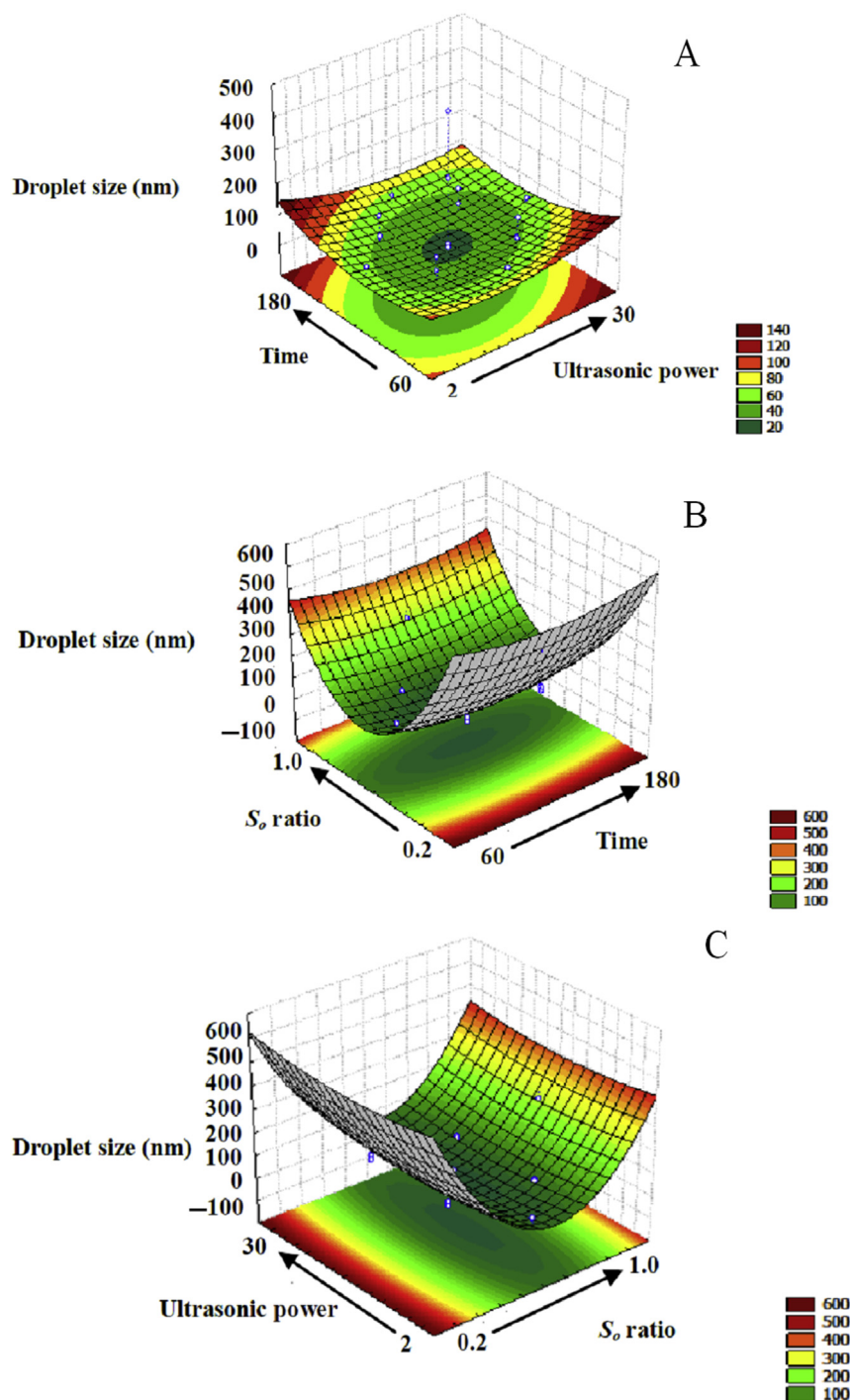


**Figure 2 – Response surface contour plot of the combined effects of  $S_o$  ratio, ultrasonic power, and ultrasonic time on droplet size of citral nanoemulsions: (A) ultrasonic power and time at constant  $S_o$  ratio (0.6); (B)  $S_o$  ratio and ultrasonic power with constant ultrasonic time (120 seconds); (C)  $S_o$  ratio and time with constant ultrasonic power (18 W).**

formed droplets [22]. In our study, when surfactants adsorb to the dispersed surface of citral, it will arrange into a suitable molecular structure. Thus, the optimal ultrasonic time would be a critical point to form the nano-scale dispersed droplet. We could obtain droplet sizes of nanoemulsions of about 100 nm at  $S_o$  ratio 0.4–0.6 and ultrasonic time 120 seconds.

Figure 2C was generated by varying the  $S_o$  ratio and ultrasonic power while maintaining the ultrasonic time at

120 seconds. We could obtain droplet sizes of nanoemulsions around of about 100 nm at  $S_o$  ratio 0.4–0.6 and ultrasonic power 18 W. The droplet size was closely related to the surfactant concentration. At low  $S_o$  ratio, not enough surfactant was available to adsorb on the surface of the newly formed droplets coalescence. Newly formed droplets are very dependent on the  $S_o$  ratio of the o/w emulsion system [9]. Initially increasing the  $S_o$  ratio results in a large decrease in droplet

size (from  $S_o$  ratio 0.2 to 0.4) because the newly formed droplets have more sufficient surfactant to be stabilized. However, increasing excess of mixing surfactant would not decrease the droplet size. In an emulsion system, much residual surfactant would interfere with the stability and appearance of emulsion. Our results agree with other studies discussing the relationship between surfactant concentration and droplet size of nanoemulsions [23].

### 3.3. TEM observation

We observed the morphology of the citral nanoemulsion formed at  $S_o$  ratio 0.6 and ultrasonic power 18 W for 120 seconds prepared with mixed surfactant at HLB 12. TEM analysis was performed with negatively stained samples. The images are shown in Figure 3: phosphotungstic acid-stained citral droplets are clearly visible, and the droplet size analysis was performed by using the Nanotract 150 light scattering instrument. In addition, the shape of the citral droplet was spherical, and the grey portion of the droplets results from the citral incorporated into the emulsion system.

### 3.4. Droplet size distribution

The droplet size distribution for citral nanoemulsions is shown in Figure 4. We found a significant passing peak between size 10 nm to 100 nm and a clear droplet-size distribution caused by the ultrasonic emulsification, which led to nanoemulsions with a small droplet size. Ultrasonic emulsions are less poly-dispersed and more stable as compared with those prepared with other mechanical devices [24].

### 3.5. Time stability of nanoemulsions stored at room temperatures

The changes in droplet size as a function of the storage time for nanoemulsions stored at room temperatures are shown in Figure 5. The droplet size increased very quickly during the

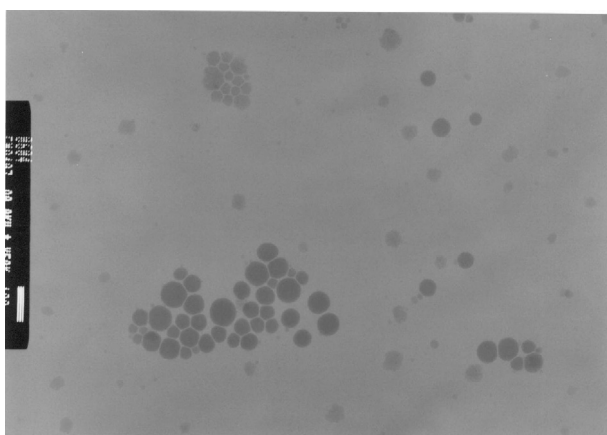


**Figure 3 – Transmission electron microscopy of droplets in citral-in-water nanoemulsion system. Scale bar, 100 nm. The emulsion was formed at  $S_o$  ratio 0.6 and ultrasonic power 18 W for 120 seconds and prepared with mixed surfactant at hydrophilic-lipophilic balance 12.**

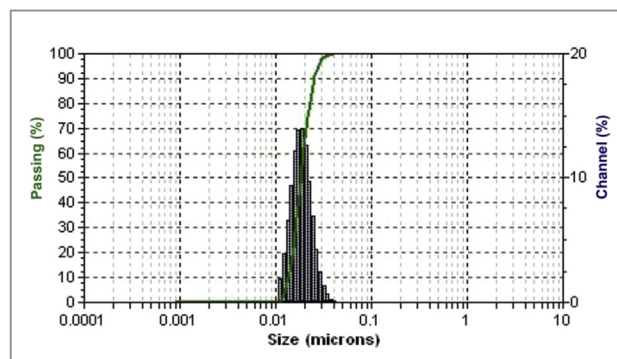


**Figure 4 – Droplet size distribution citral-in-water nanoemulsion system. The emulsion was formed at  $S_o$  ratio 0.6 and ultrasonic power 18 W for 120 seconds and prepared with mixed surfactant at hydrophilic-lipophilic balance 12.**

initial 7 days of storage at room temperatures. After 7 days, the growth rate became slower but the size was still within acceptable ranges of nanoemulsions. During the formation of droplets in the o/w emulsion system, the newly formed droplets gained more energy from the applied force, so they needed time to reach thermodynamic equilibrium [25].

### 3.6. Antimicrobial activity

Citral has the ability to disrupt and penetrate the lipid structure of the cell wall of bacteria. It leads to denaturation of protein and destruction of cell membrane followed by cytoplasmic leakage and cell lysis and death [13]. In this study, we screened the antimicrobial activity of the citral nanoemulsions formed at  $S_o$  ratio 0.6 and ultrasonic power 18 W for 120 seconds prepared with mixed surfactant at HLB 12 against six food-associated bacteria in the disk diffusion assay (Table 3). The size of the zone of inhibition is usually related to the

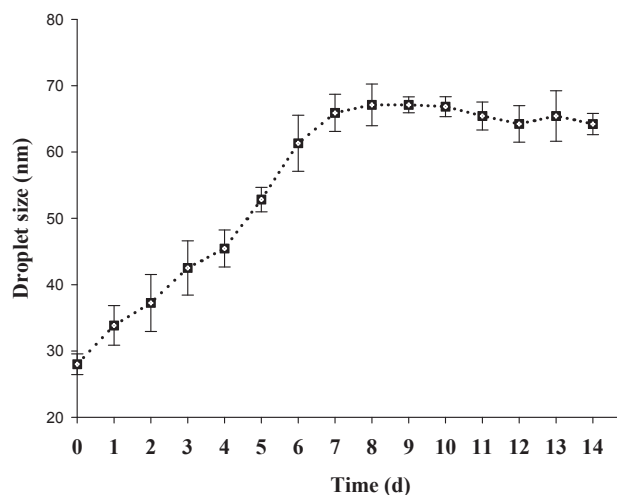


**Figure 5 – Stability of citral nanoemulsions stored at room temperature. The emulsion was formed at  $S_o$  ratio 0.6 and ultrasonic power 18 W for 120 seconds and prepared with mixed surfactant at hydrophilic-lipophilic balance 12.**

**Table 3 – Antimicrobial activity of citral nanoemulsions.**

Bacteria	Inhibition zone (mm)	
	Citral nanoemulsion	Sulphadiazine
<i>Staphylococcus aureus</i>	19.2 <sup>a</sup> ± 2.3	32 ± 0.7
<i>Escherichia coli</i>	9.4 <sup>c</sup> ± 0.5	26 ± 0.2
<i>Pseudomonas aeruginosa</i>	6.2 <sup>d</sup> ± 0.2	24 ± 0.4
<i>Enterococcus faecalis</i>	10.2 <sup>c</sup> ± 0.6	23 ± 0.8
<i>Salmonella typhimurium</i>	2.0 <sup>e</sup> ± 0.1	46 ± 1.2
<i>Listeria monocytogenes</i>	14.4 <sup>b</sup> ± 2.6	30 ± 1.1

<sup>a–e</sup> Means with different letters within the same column differed significantly ( $p < 0.05$ ). Values are mean ± standard deviation ( $n = 3$ ).

level of antimicrobial activity present in the sample or product, and a larger zone of inhibition usually means that the antimicrobial is more potent. For comparison, sulphadiazine was used as a standard. The citral nanoemulsions showed significantly different antimicrobial activities against *L. monocytogenes* and *S. aureus*. This finding agrees with previous studies of a soybean oil-based nanoemulsion that showed bactericidal properties against *Bacillus cereus*, *Bacillus subtilis*, *Haemophilus influenzae*, *Neisseria gonorrhoeae*, *Streptococcus pneumoniae*, and *Vibrio cholerae* [26].

A comparison of the antimicrobial activity of specific essential-oil nanoemulsions against Gram-positive and -negative bacteria did not reveal significant differences [27]. The nanoemulsion systems of delivery for citral likely promote their interaction with the microbial cell membranes by four main routes: (1) the increased surface area and passive transport through the outer cell membrane improves the interaction with the cyto-plasmic membranes [28]; (2) the fusion of the emulsifier droplets with the phospholipid bilayer of the cell membrane likely promotes the targeted release of the essential oils at the desired sites [29]; (3) the sustained release over time of the essential oils from the nanoemulsion droplets, driven by essential oils partition between the oil droplets and the aqueous phase, prolongs the activity of essential oils [30]; and (4) the electrostatic interaction of positively charged nanoemulsions droplets with negatively charged microbial cell walls increases the concentration of essential oils at the site of action [31]. The use of nanoscale delivery systems, such as liposome-, micelle-, micro-emulsion-, and nanoemulsion-based systems, may increase passive cellular absorption mechanisms, thus reducing mass transfer resistance and increasing antimicrobial activity [32]. In orange and pear juice systems, the addition of low concentrations of nanoencapsulated D-limonene was able to delay the microbial growth or completely inactivate the microorganisms [28].

#### 4. Conclusions

Nanoemulsion droplets can be obtained in a citral-in-water system by ultrasonic emulsification. The optimal micro-encapsulated conditions for ultrasonic emulsification of citral nanoemulsions were ultrasonic power 18 W, ultrasonic time of 120 seconds, and  $S_o$  ratio 0.4–0.6 with HLB value < 12. The citral nanoemulsions demonstrated antimicrobial activity

against bacteria. These considerations can be used for the rational design of nanoemulsion-based delivery systems for essential oils based on the desired function of the antimicrobials in the agrochemicals, cosmetics, and pharmaceuticals industries.

#### Conflicts of interest

The authors declare no conflict of interest.

#### REFERENCES

- [1] Solans C, Esquena J, Forgiarini AM, Usón N, Morales D, Izquierdo P, Azemar N, Garcia-Celma MJ. Nanoemulsions: formation, properties and applications. *J Surf Sci Series* 2003;109:525–54.
- [2] Pey CM, Maestro A, Solé I, González C, Solans C, Gutiérrez JM. Optimization of nano-emulsions prepared by low-energy emulsification methods at constant temperature using a factorial design study. *Colloid Surface A* 2006;288:144–50.
- [3] Jianguo F, Yali S, Qian Yao Y, Chencheng S, Guantian Y. Effect of emulsifying process on stability of pesticide nanoemulsions. *Colloid Surface A* 2016;497:286–92.
- [4] Sonnevile-Aubrun O, Simonnet JT, Alloret FL. Nanoemulsions: a new vehicle for skincare products. *Adv Colloid Interface Sci* 2004;108–9:145–9.
- [5] Virginia C, Marco B, Laura M, Francesco C, Michele P, Giuseppe DR. Development of nanoemulsions for topical delivery of vitamin K1. *Int J Pharm* 2016;511:170–7.
- [6] Izquierdo P, Feng J, Esquena J, Tadros TF, Dederer JC, Garcia MJ, Azemar N, Solans C. The influence of surfactant mixing ratio on nano-emulsion formation by the pit method. *J Colloid Interface Sci* 2005;285:388–94.
- [7] Saberi AH, Fang Y, McClements DJ. Fabrication of vitamin E-enriched nanoemulsions: factors affecting particle size using spontaneous emulsification. *J Colloid Interface Sci* 2013;391:95–102.
- [8] Kim DM, Hyun SS, Yun D, Lee CH, Byun SY. Identification of an emulsifier and conditions for preparing stable nanoemulsions containing the antioxidant astaxanthin. *Int J Cosmet Sci* 2012;34:64–73.
- [9] Kentish S, Wooster TJ, Ashokkumar M, Balachandran S, Mawson R, Simons L. The use of ultrasonics for nanoemulsion preparation. *Innov Food Sci Emerg* 2008;9:170–5.
- [10] Abismail B, Canselier JP, Wilhelm AM, Delmas H, Gourdon C. Emulsification by ultrasound: drop size distribution and stability. *Ultrason Sonochem* 1999;6:75–83.
- [11] Henry JVL, Fryer PJ, Frith WJ, Norton IT. Emulsification mechanism and storage instabilities of hydrocarbon-in-water sub-micron emulsions stabilized with Tweens (20 and 80), Brij 96v and sucrose monoesters. *J Colloid Interface Sci* 2009;338:201–6.
- [12] Weerawatanakorn M, Wu JC, Pan MH, Ho CT. Reactivity and stability of selected flavor compounds. *J Food Drug Anal* 2015;23:176–90.
- [13] Amna AS, Suzan AK. Chemical and antimicrobial studies of monoterpene: citral. *Pestic Biochem Phys* 2010;98:89–93.
- [14] Jun-Hyung T, Murray BI. Metabolism of citral, the major constituent of lemongrass oil, in the cabbage looper, *Trichoplusia ni*, and effects of enzyme inhibitors on toxicity and metabolism. *Pestic Biochem Phys* 2016;133:20–5.
- [15] Nishijima CM, Ganey EG, Mazzardo-Martins L, Martins DF, Rocha LR, Santos AR, Hiruma-Lima CA. Citral: a

- monoterpene with prophylactic and therapeutic anti-nociceptive effectiveness in experimental models of acute and chronic pain. *Eur J Pharmacol* 2014;736:16–25.
- [16] He X, Hwang HM. Nanotechnology in food science: functionality, applicability, and safety assessment. *J Food Drug Anal* 2016;24:671–81.
- [17] Qiaobin H, Hannah G, Indu U, Kumar V, Yangchao L. Antimicrobial eugenol nanoemulsion prepared by gum Arabic and lecithin and evaluation of drying technologies. *Int J Biol Macromol* 2016;87:130–40.
- [18] Moghimi R, Aliahmadi A, McClements DJ, Rafati R. Investigations of the effectiveness of nanoemulsions from sage oil as antibacterial agents on some food borne pathogens. *LWT-Food Sci Technol* 2016;71:69–76.
- [19] Soottitantawat A, Yoshii H, Furuta T, Ohkawara M, Linko P. Microencapsulation by spray drying: influence of emulsion size on the retention of volatile compounds. *J Food Sci* 2003;68:2256–62.
- [20] Meynier A, Lecoq C, Genot C. Emulsification enhances the retention of esters and aldehydes to a greater extent than changes in the droplet size distribution of the emulsion. *Food Chem* 2005;93:153–9.
- [21] Jafari SM, He Y, Bhandari B. Production of sub-micron emulsions by ultrasound and microfluidization techniques. *J Food Eng* 2007;82:478–88.
- [22] Jena S, Das H. Modeling of particle size distribution of sonicated coconut milk emulsion: effect of emulsifiers and sonication time. *Food Res Int* 2006;39:606–11.
- [23] Liu W, Sun D, Li C, Liu Q, Xu J. Formation and stability of paraffin oil-in-water nano-emulsions prepared by the emulsion inversion point method. *J Colloid Interface Sci* 2006;303:557–63.
- [24] Lin CY, Chen LW. Emulsification characteristics of three- and two-phase emulsion prepared by the ultrasonic emulsification method. *Fuel Process Technol* 2006;87:309–17.
- [25] Nazarzadeh E, Anthonypillai T, Sajjadi S. On the growth mechanisms of nanoemulsions. *J Colloid Interface Sci* 2013;397:154–62.
- [26] Laura S, Alejandra R, Robert S, Olga M. Physicochemical characterization and antimicrobial activity of food grade emulsions and nanoemulsions incorporating essential oils. *Food Hydrocolloids* 2015;43:547–56.
- [27] Donsì F, Ferrari G. Essential oil nanoemulsions as antimicrobial agents in food. *J Biotechnol* 2016;233:106–20.
- [28] Donsì F, Annunziata M, Vincenzi M, Ferrari G. Design of nanoemulsion-based delivery systems of natural antimicrobials: effect of the emulsifier. *J. Biotechnol* 2012;159:342–50.
- [29] Li W, Chen H, He Z, Han C, Liu S, Li Y. Influence of surfactant and oil composition on the stability and antibacterial of eugenol nanoemulsions. *LWT-Food Sci Technol* 2015;62:39–47.
- [30] Majeed H, Liu F, Hategekimana J, Sharif HR, Qi J, Ali B, Bian YY, Ma J, Yokoyama W, Zhong F. Bactericidal action mechanism of negatively charged food grade clove oil nanoemulsions. *Food Chem* 2016;197:75–83.
- [31] Chang Y, McLandsborough L, McClements DJ. Fabrication, stability and efficacy of dual-component antimicrobial nanoemulsions; essential oil (thyme oil) and cationic surfactant (lauric arginate). *Food Chem* 2015;172:298–304.
- [32] Donsì F, Annunziata M, Sessa M, Ferrari G. Nanoencapsulation of essential oils to enhance their antimicrobial activity in foods. *LWT-Food Sci Technol* 2011;44:1908–14.